Chapter 4: Model setup

This chapter describes the modelled heat exchangers' geometric characteristics and simulation setup in detail. It has the following structure:

- Steady-state simulations:
  - Model geometry
  - Mesh generation
  - Boundary conditions
  - Physics models
  - Relaxation
  - Convergence
  - Hardware
- Transient multiphase simulations:
  - Geometry
  - Mesh generation
  - Boundary conditions
  - Physics models
  - Relaxation

A thorough discussion on the geometrical parameters, calculations and variations between designs for both the steady-state and transient multiphase simulations are presented. The chapter starts with a discussion on the general geometrical parameters of the STHEs that were modelled in the current study, including an examination of the geometric information that was relevant to the specific configurations. A segment on the meshing methodology and parameters is presented, followed by a basic exposition of the important simulation input requirements. A brief discussion is provided on the conventions behind convergence and the hardware that was used. This breakdown is presented for both the steady-state and transient multiphase simulations, finishing with the conclusion.

4.1. Steady-state simulations

The requirements for the setup of the steady-state simulations are discussed in this section.

4.1.1. Model geometry

As discussed in Chapter 2.1, the heat exchangers under consideration are of AEL construction. General geometry parameters of the heat exchanger obtained from the Sasol general arrangement drawings are:

- Shell inner diameter is 910 mm.
- Shell length is 6070 mm.
- Inlet/Outlet nozzle inner diameter is 430 mm.
- Inlet nozzle's central axis is placed 450 mm from tube-sheet face.
- The outlet nozzle's central axis is placed 510 mm from the tube-sheet face.
- 600 and 556 tubes are used.
- Tube pitch is 32 mm.
- Tube outer diameter is 25 mm.
- Tubes are placed 22 mm from shell centrelines.
- Six baffle plates (seven compartments) are used.
- Baffle plate thickness is 10 mm.
- Inter-baffle spacing is 858 mm.
- Baffle-tube-sheet spacing is 890 mm.
- Symmetry plane is assumed to lie on the heat exchanger centreline.

Some components that have been discussed in Chapter 2 were omitted from the design, namely:

- two pairs of sealing strips – in order to observe the influence of the bundle-shell bypass stream better;
- the baffle rod supports – for simplicity;
- nozzle connections – for simplicity; and
- baffle-shell and baffle-tube manufacturing clearances – clearances are too small to allow for effective mesh generation in these regions whilst staying within memory capabilities.

The most important geometric features are shown in Figure 20 below. The inlets and outlets are consistently shown in a green and a red hue, respectively, with baffles and tube-sheet internal surfaces being shown in yellow.

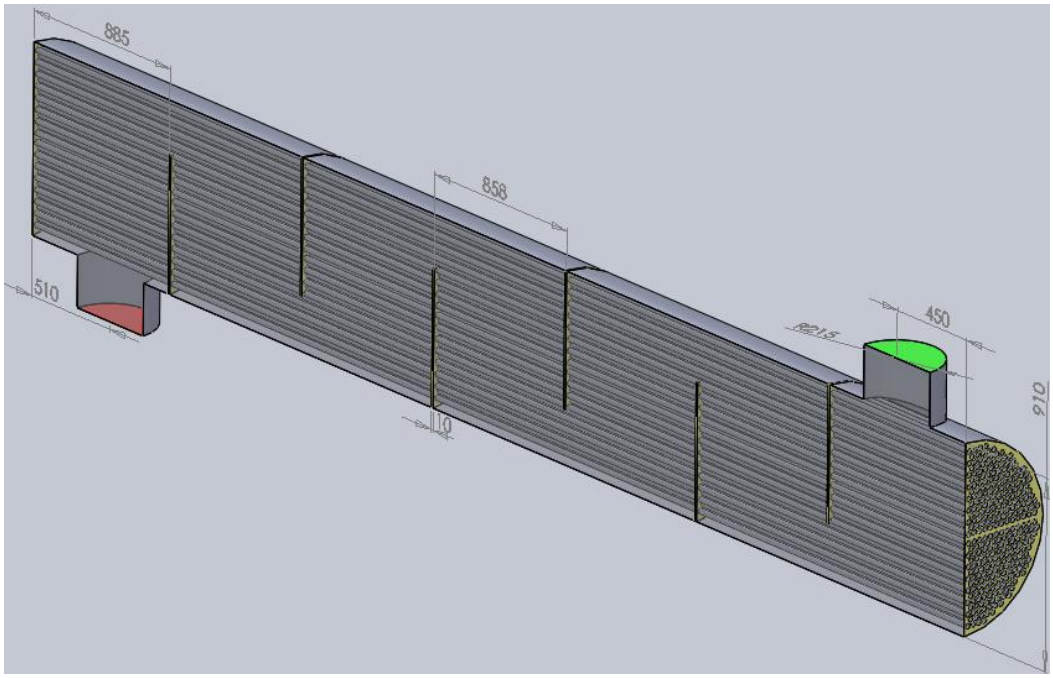

Figure 20: Steady-state heat exchanger geometry

Tube layout

As shown and discussed in Chapter 1.3, tubes can have four different configurations that are measured relative to the incoming stream direction, namely 30°, 45°, 60° and 90° (Figure 3), of which the square (90°) and rotated triangular (30°) configurations have been selected. The pitch, size and centre tube row placement of all configurations are consistent; however, the square arrangement results in a total of 278 tubes per half where the rotated triangular array has 300 tubes per half.

Baffle layout

The baffle configurations that have been selected for simulations are the single-segmental, double-segmental and disc-and-doughnut baffles that are shown in Figure 1. A consistent cross-sectional baffle-cut area is retained throughout the configurations. The calculation is based on the free flow area of a single-segmental baffle and the equivalent area, and the

subsequent geometry, was calculated for the double-segmental and disc-and-doughnut configurations. Functionality within the drawing software package Solidworks was used to calculate the baffle flow areas.

The single-segmental baffle geometry was obtained from the heat exchanger general arrangement drawings. The drawings have been omitted from the appendices due to the proprietary content. The baffle-cut is 652.75 mm (72%), measured from the shell to the edge of the baffle centreline (Figure 21).

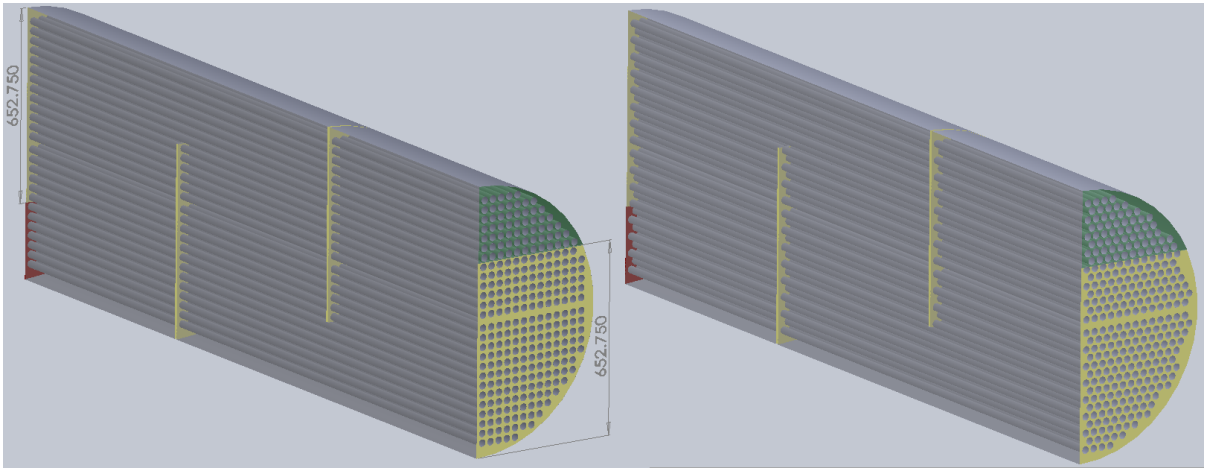

Figure 21: Sections of 90° and 60° single-segmental configurations

The geometry that was calculated for the Double_60 and Double_90 configurations respectively places the inner edge of the peripheral baffle sections 91 mm and 77 mm from the centreline and the edges of the central section 307.5 mm and 305 mm from the centreline (Figure 22).

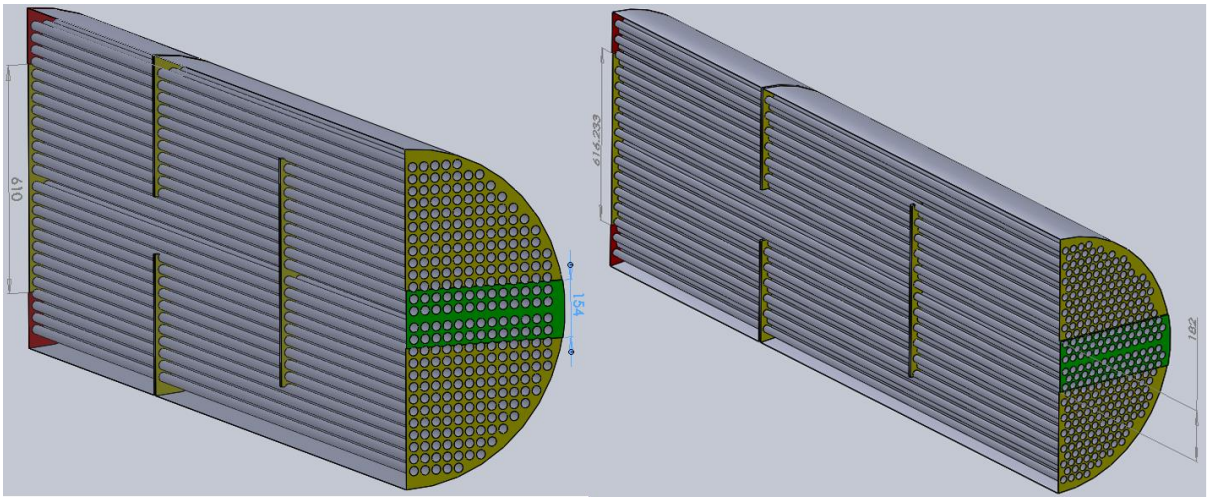

Figure 22: Sections of 90° and 60° double-segmental configurations

The geometry that was calculated for the DnD_60 and DnD_90 configurations respectively places the internal edge of the doughnut sections at a radius of 234 mm and 225 mm and the external edge of the central disc sections at a radius of 419.5 mm and 415 mm (Figure 23).

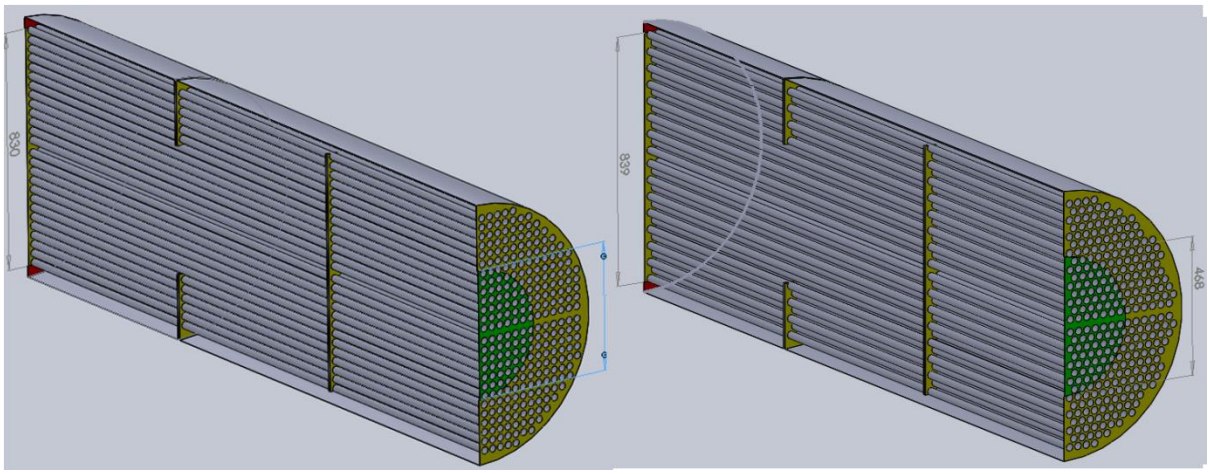

Figure 23: Sections of 90° and 60° disc-and-doughnut configurations

The different configurations were divided into three sections each, resulting in 18 separate simulations. Reasons behind the segmentation are discussed later on in the chapter. The naming convention that was used to describe the simulations firstly indicates the baffle configuration, secondly the tube arrangement and lastly the section number of the heat exchanger, as indicated in Table 5.

Single-segmental configuration	Double-segmental configuration	Disc-and-doughnut configuration
Rotated triangular array	Rotated triangular array	Rotated triangular array
Single_61	Double_61	DnD_61
Single_62	Double_62	DnD_62
Single_63	Double_63	DnD_63
Square array	Square array	Square array
Single_91	Double_91	DnD_91
Single_92	Double_92	DnD_92
Single_93	Double_93	DnD_93

Table 5: Naming conventions of simulations

4.1.2. Mesh generation

STAR-CCM+ has a selection of three types of core mesh elements: hexahedral, tetrahedral and polyhedral. The latter is the selected option due to the following reasons: polyhedral cells have effortless generation characteristics and convergence behaviour (Spiegel *et al.,* 2010:14; STAR-CCM+ User Guide v.6.06, 2011:1798).

By selecting polyhedral cells as the core element of mesh generation, the difficulties that are experienced by tetrahedral and hexahedral cells with regard to a limited number of neighbouring cells are eliminated. A polyhedral cell can have an average of 14 faces, leading to better gradient approximations across all faces. In regions of planar generation, in other words boundaries, polyhedral cells have a sufficient number of neighbouring cells, resulting in accurate gradient and flow distribution calculations (Peric & Ferguson, 2005:1).

Comparing elements with respect to the number of cells, polyhedral meshes can have a fourth of the number of cells, half the memory usage and between a fifth and a tenth of the computing time requirements (Peric & Ferguson, 2005:1).

STAR-CCM+ provides the user with a selection of quantifiable attributes that define cell size within a mesh. The four most important attributes/factors are discussed below.

Cell base size

This is the parameter on which the mesh generation process is based and determines the general size of an element in the mesh. Other parameters are either specified relative to this value or can be user defined.

Prism layer thickness

Prism layer cells are generated on the wall boundaries to ensure a well-organized, prismatic mesh for the solution of the boundary layer. The default number of prism layer cells (2) was used for the simulations. The specified thickness (relative or absolute) defines the total height of the generated prism cells. Prism layer stretching is another factor that influences the generation of the prismatic cells. A stretch factor of 1.5 is the default value which calculates the cell thickness, based on a ratio between the cell and the neighbouring cell that is closer to the wall.

Relative minimum size

This parameter defines the minimum size of the generated cell faces. In order to retain adequate cell quality, one should consider the minimum distance between boundary faces and ensure that the specified value is smaller.

Relative target size

This parameter determines the target size for all cell faces. If the target size does not fit within the boundaries, it will be refined successively up to the relative minimum size.

Mesh parameter values

In order to capture the flow within the heat exchanger effectively, the mesh had to be sufficiently fine. The minimum distance between tube surfaces is 7 mm. The base and target size for all simulations were selected as 10 mm and taking into account the height of the 1 mm prism layers, a minimum cell size of 4 mm was able to capture the flow in between the tubes sufficiently. The values of these parameters have been validated to give a sufficiently fine mesh resolution by means of a mesh independence study, the results of which are presented and discussed in Chapter 5.1. The choice of these values resulted in the mesh size for an entire configuration being roughly 32 million to 42 million cells, rendering the available computing resources inadequate; the geometry was thus divided into sections that were small enough to fit within the computational capacity, whilst retaining an accurate representation of the geometry without having to make simplifying assumptions. This will similarly allow and accurate representation of the flow field and characteristics within these small spaces.

The heat exchangers were subsequently divided into three sections, consisting of the first and last two compartments, separated by the middle three. The section plane was placed in the middle of each baffle, designating new outlets and inlets for all sections. In order to preserve continuity, the values of velocity, turbulent kinetic energy and turbulent dissipation rate were extracted at the outlet of the first section and imported as the inlet values for the

next. The section planes are shown below, indicated by the blue rectangles (Figure 24). It is inevitable that upstream effects will not be captured, due to the nature of the solution methodology. The only way to quantify the effect would be to simulate a simplified heat exchanger fully and segmentally and compare the results.

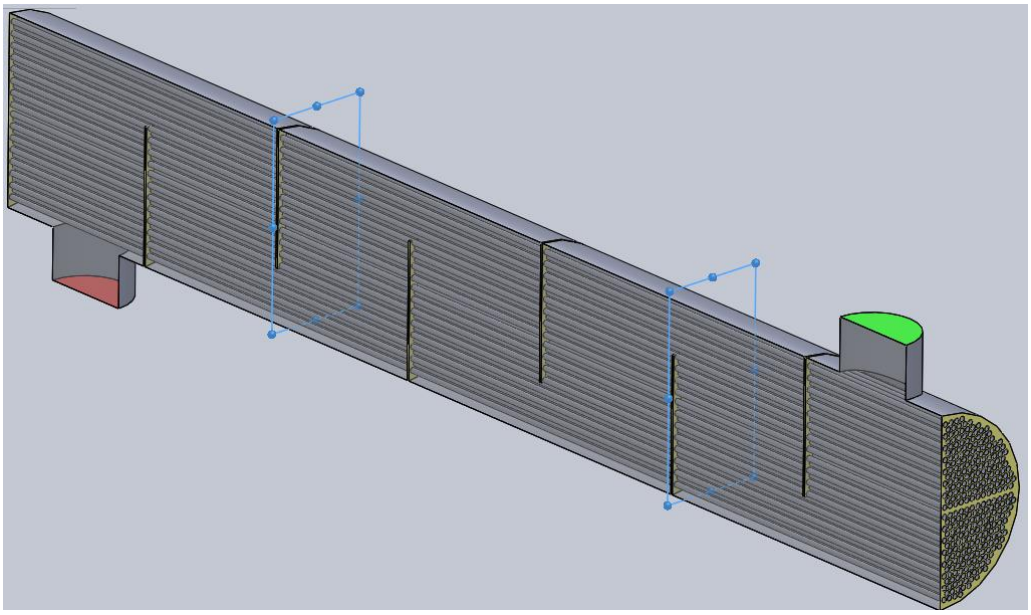

Figure 24: Plane sections indicating configuration sections

The number of cells for each section of the configuration models is tabulated below:

Simulation mesh sizes					
Single_61	9369395	Double_61	11517440	DnD_61	10850200
Single_62	13315610	Double_62	17136390	DnD_62	16989630
Single_63	9349886	Double_63	11532270	DnD_63	11477120
Single_91	9477506	Double_91	11759770	DnD_91	11782530
Single_92	13340020	Double_92	18193240	DnD_92	17029760
Single_93	9514062	Double_93	12113210	DnD_93	12417260

Table 6: Mesh sizes for the 18 models

A detailed view of the generated mesh structures for both the square and rotated triangular tube layout is presented in Figure 25 to Figure 28. A clear illustration of the prismatic and polyhedral cells between boundaries is visible and captures the geometry efficiently.

Figure 25: Generated mesh for the rotated triangular tube configuration

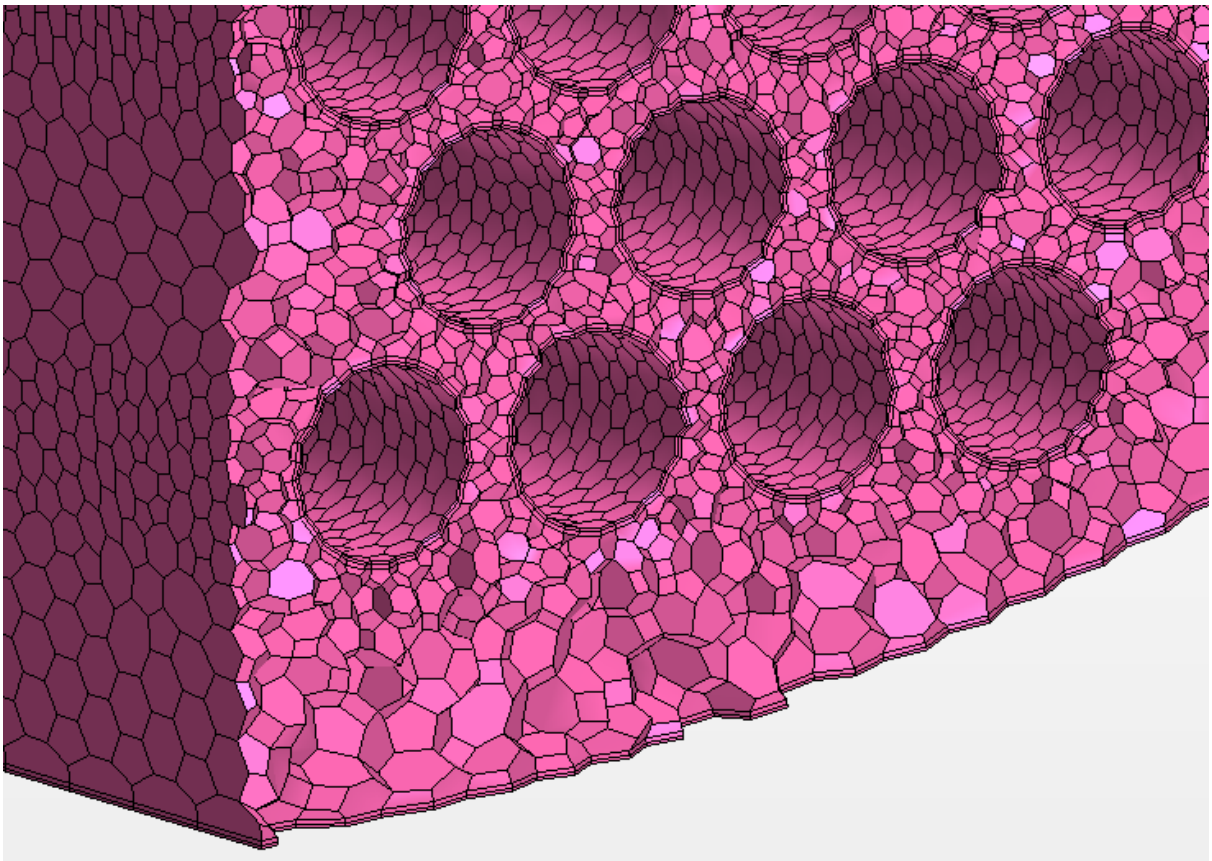

Figure 26: Detailed view of the generated mesh for the rotated triangular tube configuration

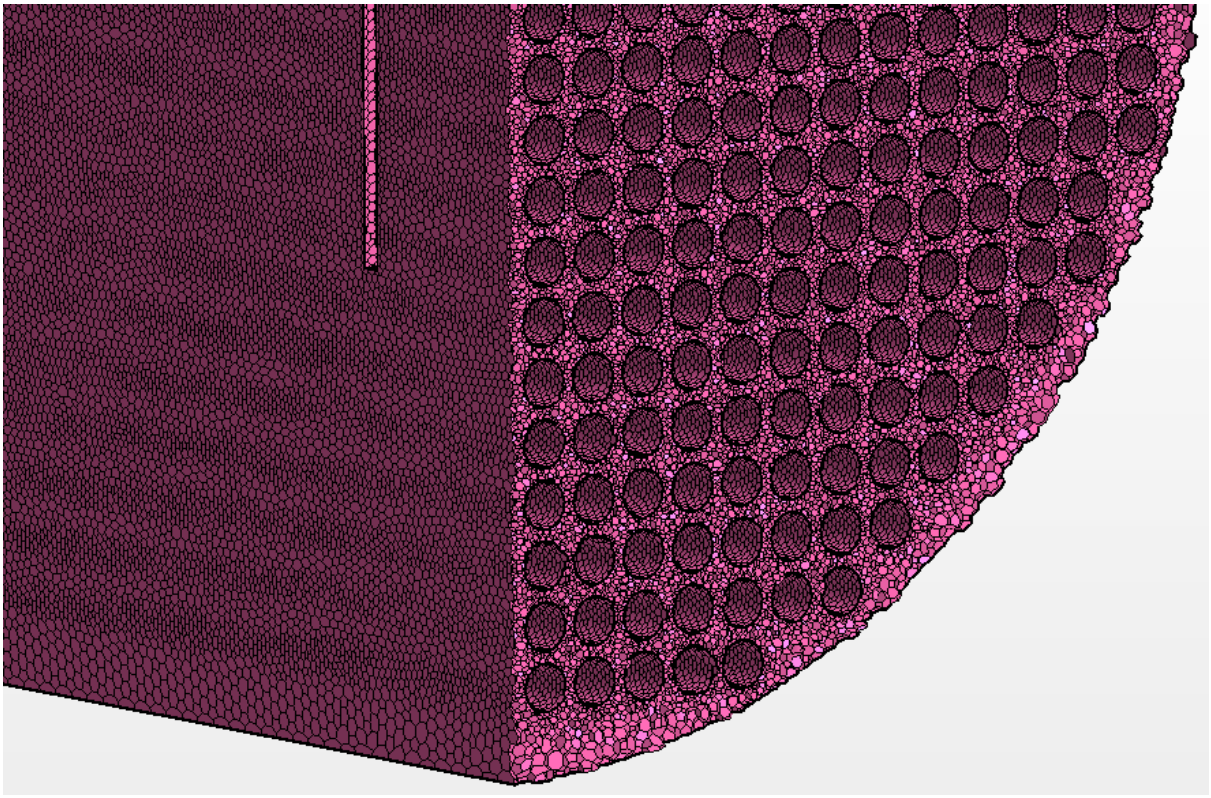

Figure 27: Generated mesh for the square tube configuration

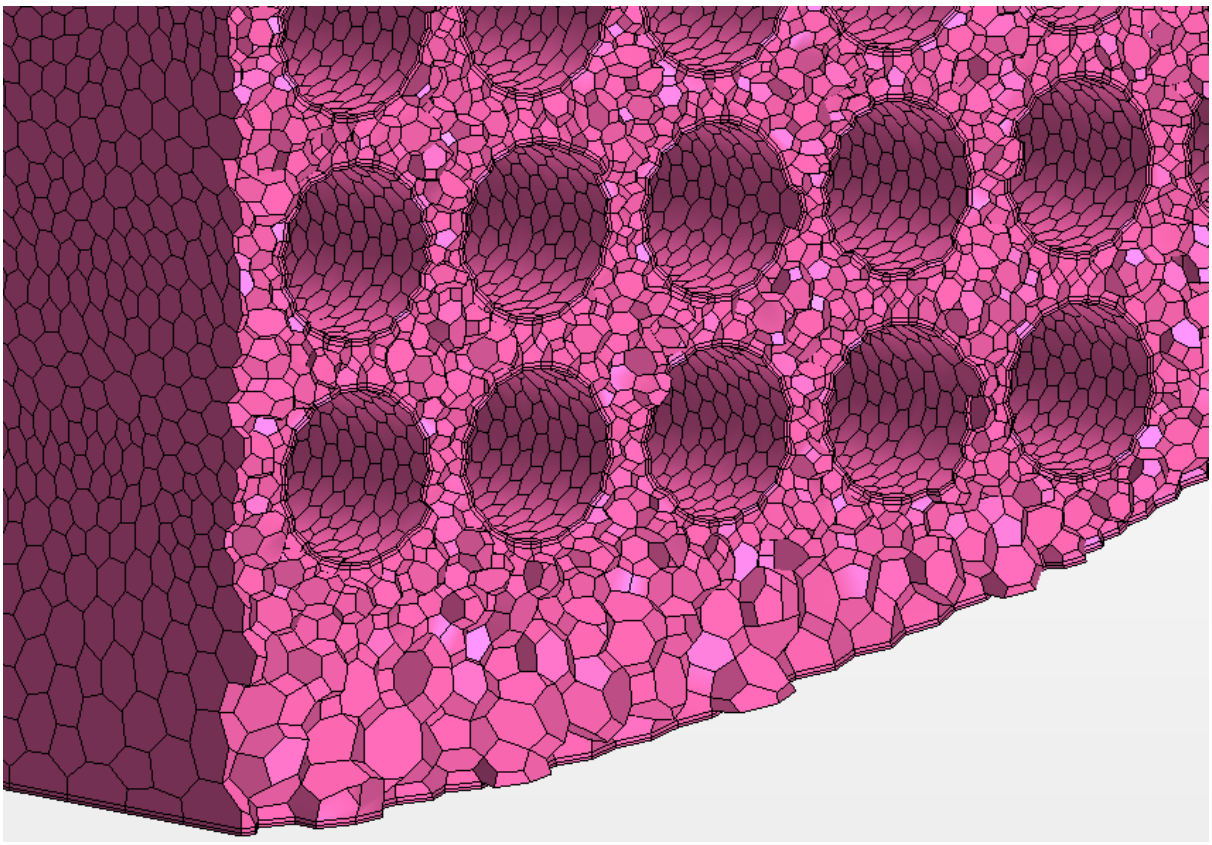

Figure 28: Detailed view of the generated mesh for the square tube configuration

4.1.3. Boundary conditions

For the simulation, four different types of boundaries were specified: symmetry plane, wall boundaries, inlet and outlet.

As discussed earlier in this chapter, the heat exchanger is symmetrical around a plane through its vertical axis and the flow is consequently assumed to be symmetrical about the plane; the face of the central vertical section plane was thus chosen as a symmetry plane.

The shell, baffle and pipe walls were logically defined as wall boundaries. The prism layer cells were generated on these surfaces within which the boundary layer flow was resolved.

The inlets of the sections were defined as velocity boundaries. The velocity over the boundary was user defined or fixed, whereas the pressure was free to fluctuate. The inlet velocities of the steady-state simulations were fixed at 1 m/s and the middle and last sections' velocity, turbulent dissipation rate and kinetic energy distributions were imported from the outlets of the initial and middle sections respectively.

The outlets of the sections were defined as pressure boundaries. In these cases, the pressure at a boundary was user defined and fixed, with the velocity free to fluctuate. The static pressure head distribution in the heat exchanger had quite a large influence on the flow and solution behaviour of the simulations and had to be fixed. The static pressure distribution was specified as the outlet pressure, but did not influence the total pressure over the outlet, as dynamic pressure was free to fluctuate. The default values of all other outlet variables were retained.

4.1.4. Physics models

STAR-CCM+ requires a selection of different physics models in order to model the relevant flow characteristics within the geometry effectively. The selected method of modelling space, time and material for the steady-state simulations are presented in Table 7.

Category	Selection
Space	Three-dimensional
Time	Steady-state
Material	Liquid
Flow	Segregated flow
Equation of state	Constant density
Viscous regime	Turbulent
Reynolds-averaged turbulence	K-ε turbulence
K-ε turbulence	Realizable k-ε model two-layer
Optional models	Gravity
	Cell quality remediation

Table 7: Physics model selection

All but two of the selected models have either been discussed in some way or are logically justifiable.

The segregated flow model solves the equations for velocity and pressure in an uncoupled manner, linking the continuity and momentum transport equations by means of the SIMPLE algorithm. The STAR-CCM+ User Guide v.6.06 confirms the use thereof for constant density flows (2011:2463).

Cell quality remediation is a method of lessening the impact of poor cell quality on the accuracy of the solution. Based on predetermined criteria, the software identifies poor quality cells and modifies gradients of the cell and its neighbours in order to improve robustness of the solution.

4.1.5. Relaxation

Solution of the equations is an iterative process. The convergence behaviour of the solution can be controlled by means of under-relaxation parameters. The under-relaxation parameter is user specified (between 0 and 1) and defined as the degree to which the previous solution results are replaced by the newly determined results (STAR-CCM+ User Guide v.6.06, 2011:678). In the simulations, the parameters for velocity, pressure, k-ε turbulence and k-ε turbulent viscosity could be adjusted. The under-relaxation parameters for all simulations were not consistent, but dependent on the solution convergence behaviour up to a point. Values were generally in the range of 0.5 for the first and second parameters and below 0.3 for the latter and increased to between 0.9 and 0.7 as the simulation progressed, in order to accelerate the solution convergence.

4.1.6. Convergence

Convergence in STAR-CCM+ is usually determined by residual monitors and a user-initialised/defined force or pressure coefficient for final convergence. STAR-CCM+ provides only the first and second order upwind discretization methods for simulations using RANS turbulence models, of which the latter is selected in the present study. Residuals are the remainders of these solved discretized equations and the values are root-mean-square averaged (STAR-CCM+ User Guide v.6.06, 2011:4930). The residuals of the continuity equation, the x-, y- and z-momentum equations, the turbulent kinetic energy and turbulent dissipation rate are monitored and plotted by default. General convergence of the simulations was determined by ensuring that the mentioned variables' residuals decrease to below 1E-3.

For final convergence, the pressure drop values over the section were monitored. Simulations were deemed converged if the pressure drop was stabilized and if it varied by less than 0.1 Pascal per iteration under less stringent under-relaxation.

4.1.7. Hardware

The steady-state heat exchangers were modelled by using STAR-CCM+ v.7.02. The hardware that was used for the simulations is an Intel I7 with a 3.4 GHz processor which ran at 3 cores; three 8 GB third generation destination data register (DDR 3), 1667 MHz RAM modules and an Nvidia GeForce GT 440 graphics card with a 1 GB RAM.

4.2. Transient multiphase setup

4.2.1. Geometry

The geometry and mesh for the transient multiphase simulations had to be re-evaluated. Due to the resource-consuming nature of the simulation, the notion of simulating multiple sections of one heat exchanger had to be discarded. Mitigation of this situation resulted in the selection of the first four compartments of the heat exchanger, omitting the last three entirely. The choice was based on the assumption that the majority of the deposition of particles will be concentrated in the first four compartments and that transportation of

sediment downstream will only commence after significant deposits have already formed in the initial compartments.

The geometry was simplified to further alleviate the strain on computational resources. The number of tubes was reduced to 100 and 90 for the rotated triangular and square tube configurations, respectively. Due to the unfeasibility of simulating the actual geometry, the simplified geometry would only be simulated to examine and compare the trends observed in shell-and-tube heat exchangers, which would be reasonably similar, regardless of the geometry.

The geometries are shown in Figure 29 and Figure 30. Once again, the inlets are shown in a green hue and the outlets in red.

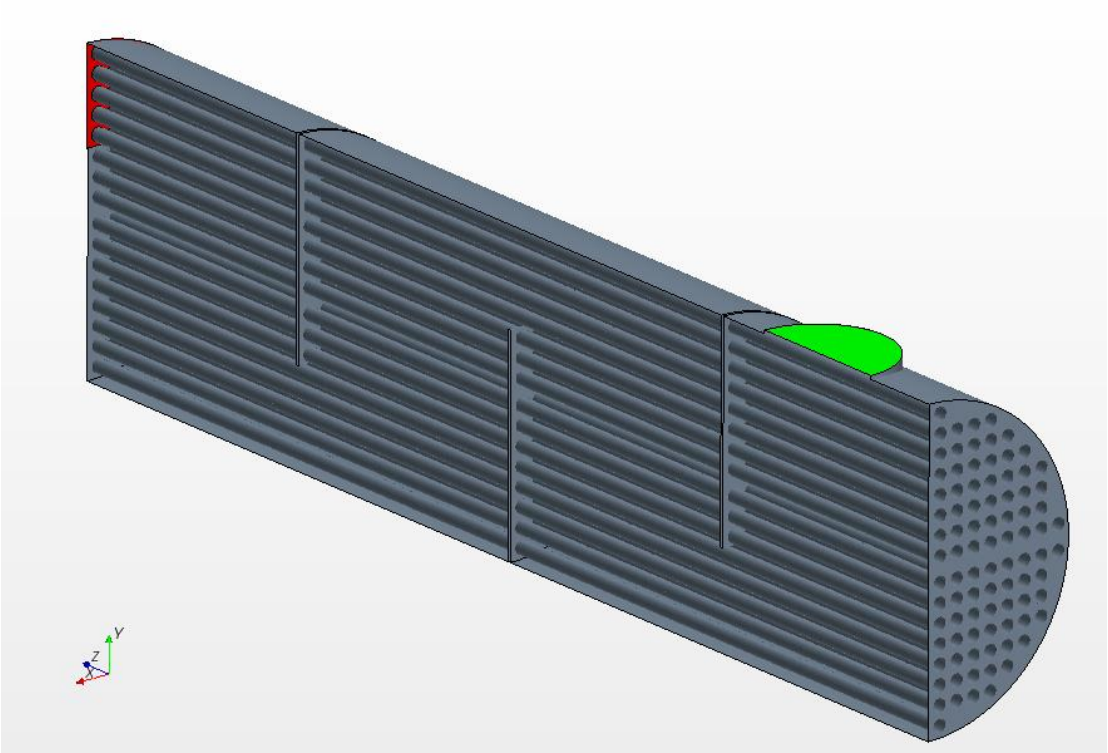

Figure 29: Geometry of the multiphase square tube configuration

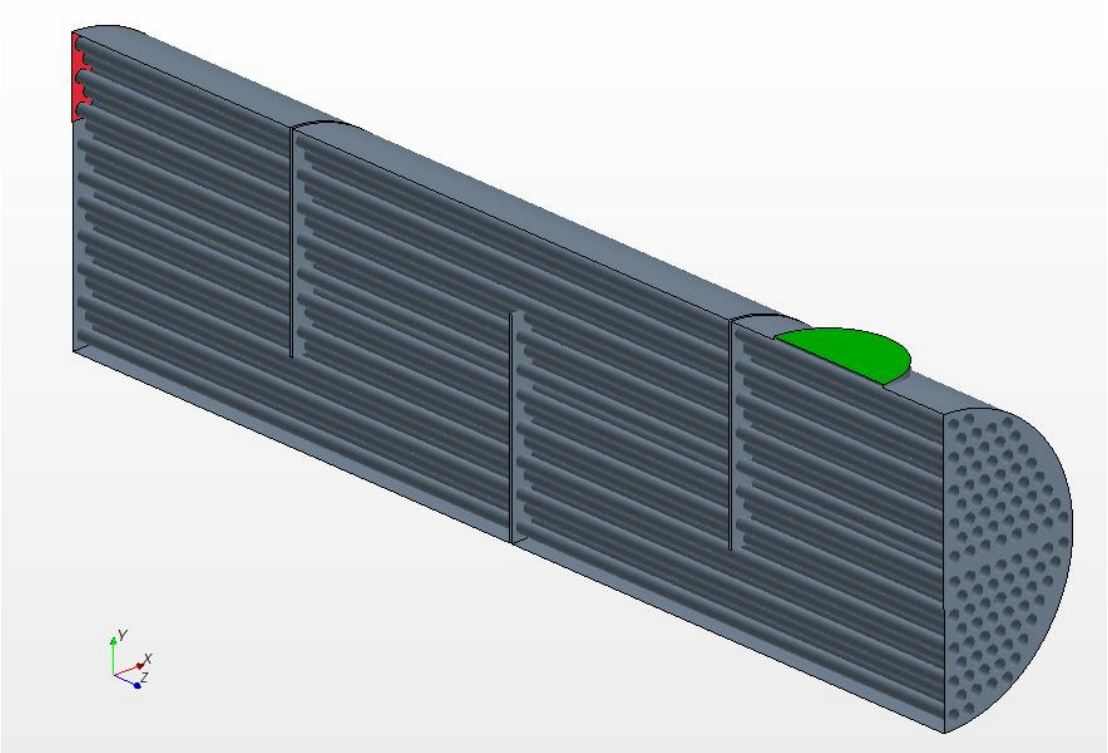

Figure 30: Geometry of the multiphase rotated triangular tube configuration

The geometrical parameters for the multiphase simulations are the following:

- Shell inner diameter is 910 mm.
- Shell length is 3420 mm.
- Inlet nozzle inner diameter is 430 mm.
- Inlet nozzle central axis is placed 450 mm from tube-sheet face.
- 100/90 tubes are used.
- Tube pitch is 55 mm.
- Tube outer diameter is 41 mm.
- Tubes are placed 36 mm from shell centrelines.
- Three baffle plates (four compartments) are used.
- Baffle plate thickness is 10 mm.
- Inter- baffle spacing is 858 mm.
- Baffle-tube-sheet spacing is 830 mm.
- Symmetry plane is once again assumed on the heat exchanger centreline.

4.2.2. Mesh generation

Having dealt with the geometry, the mesh size created further complications. The steady-state simulations' mesh resolution would inevitably have been too computationally strenuous, thus the overall size was reduced by increasing the base, prism layer, minimum and target sizes to 25 mm, 6 mm, 8.5 mm and 62.5 mm, respectively. The parameter values have also been validated by means of a mesh independence study, discussed in Chapter 5.1. These parameter values resulted in the simulations having a mesh size of 2 643 218 and 2 973 626 cells for the rotated triangular and square configurations, respectively. The mesh representations are shown from Figure 31 to Figure 34.

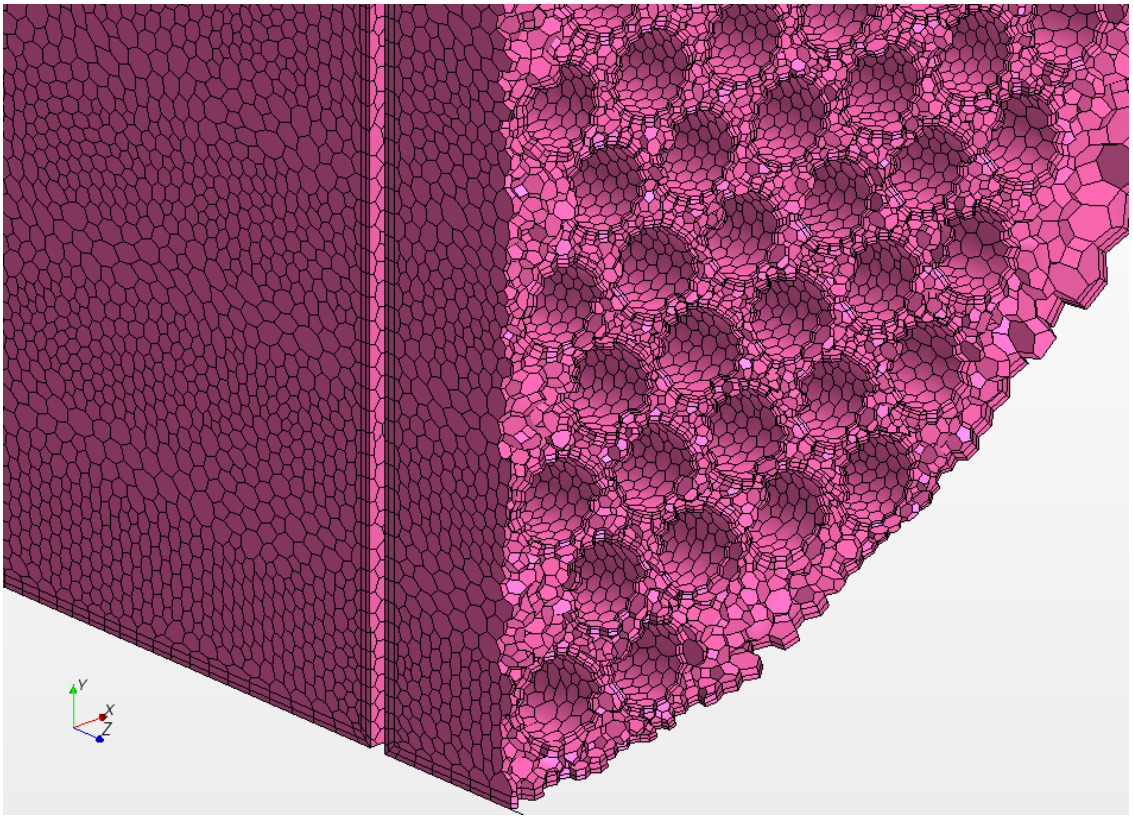

Figure 31: Generated mesh for the multiphase rotated triangular tube configuration

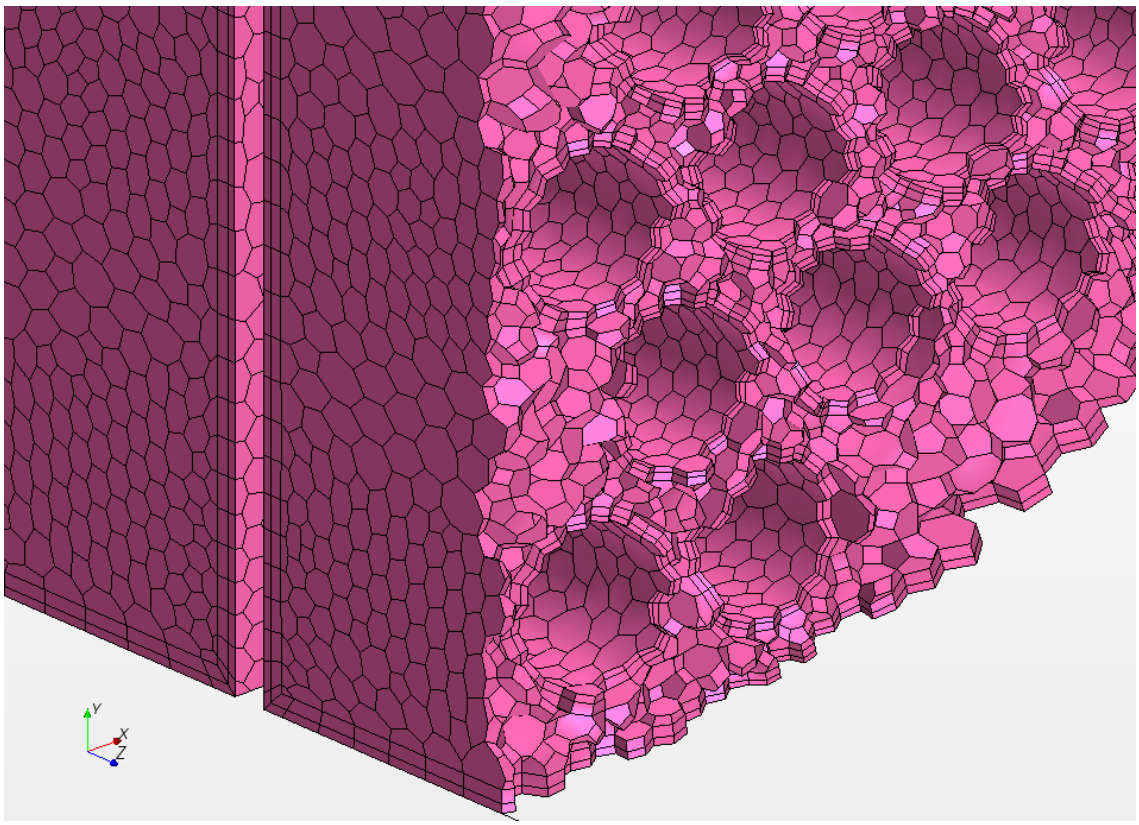

Figure 32: Detailed view of the generated mesh for the multiphase rotated triangular tube configuration

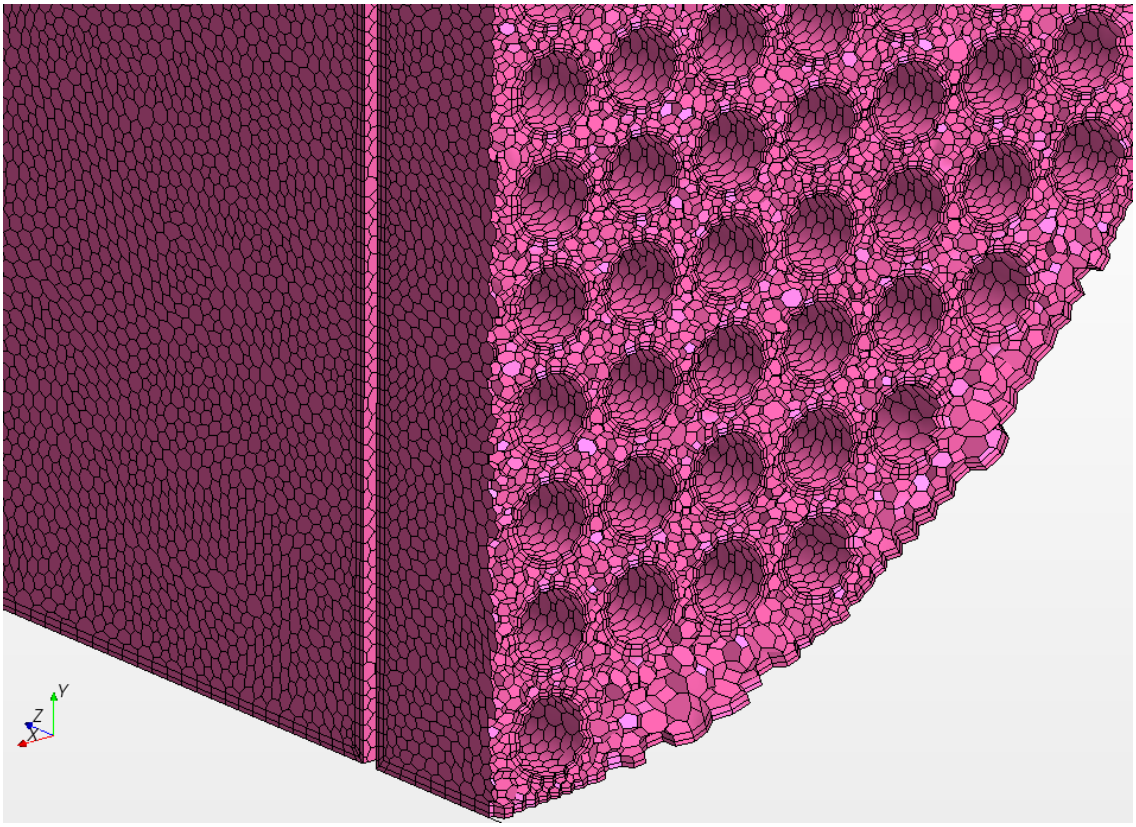

Figure 33: Generated mesh for the multiphase square tube configuration

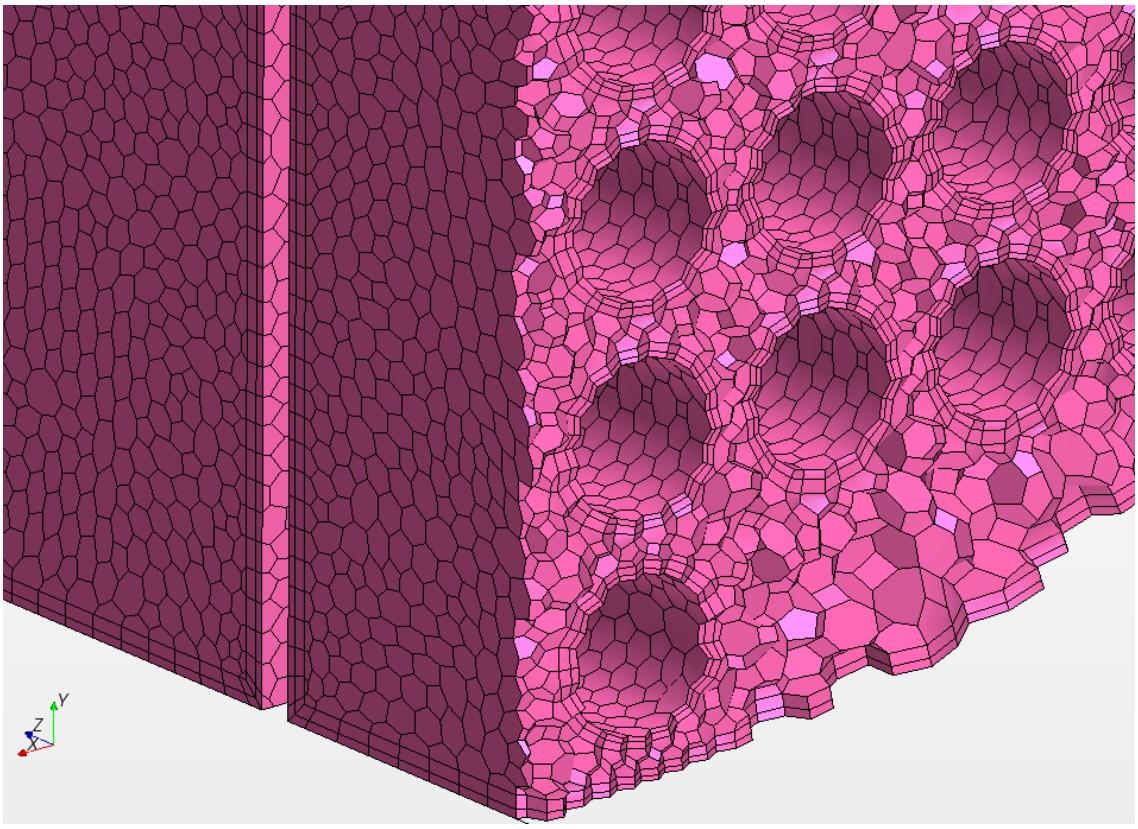

Figure 34: Detailed view of the generated mesh for the multiphase square tube configuration

4.2.3. Boundary conditions

Boundary values

The boundary values for the multiphase simulations are practically the same as for the steady-state simulations. In order to increase the stability characteristics of the simulations, the inlet velocity was reduced to 0.9 m/s and the outlet boundaries were selected as flow split outlets, where velocity and pressure are both free to fluctuate.

Sedimentation

As mentioned in Chapter 1.1, corrosion product, ash, char and slag particles are possibly entrained within the process stream, although the exact composition of the mixture is unknown. Consequently, it is assumed that the sediment can be modelled as brick (fired clay) particles with the mixture dynamic viscosity of 1.0E-6 and a density of 2645 kg/m^3, the particle size is assumed to be 1 mm and the concentration of sediment flowing into the heat exchanger is 30% by volume.

4.2.4. Physics models

The selected physics models for the multiphase simulations differ from that of the steady-state simulations.

Category	Selection
Space	Three-dimensional
Time	Implicit unsteady
Material	Multiphase mixture
Multiphase flow model	Multiphase segregated flow
Equation of state	Constant density
Viscous regime	Turbulent
Reynolds-averaged turbulence	K-ε Turbulence
K-ε turbulence models	Multiphase standard k-ε two-layer model
Optional models	Gravity
	Cell quality remediation
	Solid pressure force

Table 8: Physics model selection for the multiphase simulations

The implicit unsteady model is the only transient solver that is available with the segregated and turbulent flow models. The model enables the user to specify the time step to be used in the simulation, among other parameters.

Transient analysis

For the multiphase simulations, it is required to have a visual representation of the sediment concentration distribution throughout the heat exchanger at different instances in order to compare the effectiveness of the two configurations. Owing to the unstable nature of the simulations, small time steps and heavy under-relaxation of variables were required to enable and enhance simulation convergence. A time step of 1E-3 second (1 millisecond) has been selected, based on the convergence behaviour exhibited.

The software's transient solution procedure is to solve the flow field internally for one time step, using the results as the initial conditions of the next. The number of internal iterations for each time step also determines the level of convergence that is obtained per time step.

150 internal iterations were assumed to be sufficient to solve the equations within a time step to a sufficient level of convergence, whilst retaining a satisfactory balance between accuracy and overall solution time. This assumption has been proven by several preliminary simulations, which are, however, not presented in the present text.

Standard k-ε model

The multiphase standard k-ε model is the only available turbulence model for multiphase mixtures. As discussed in Chapter 2.5, it presents some difficulties with regard to accuracy and stability. These difficulties are, however, not of dire importance for the multiphase flow simulations, considering that the same range of discrepancies will be observed and compared and are thus assumed to be negligible. The geometries have also been modified from the original design parameters in order to highlight certain trends between the configurations.

4.2.5. Relaxation

The general relaxation parameters that are used for the steady-state simulations were too moderate for use in multiphase flow analysis. Multiphase flow is generally more unstable, further complicated by the addition of transient analysis and the choice of turbulence modelling; thus, the relaxation parameters had to be adjusted in order to compensate for this instability. The following values were used.

Parameter	Under-relaxation value
Coupled phase velocity	0.015
Turbulent dissipation	0.025
Pressure	0.025
Volume fraction	0.05
Multiphase k-ε turbulence	0.025
Turbulent viscosity	0.1

Table 9: Under-relaxation values for the multiphase simulations

4.2.6. Hardware

The multiphase simulations were completed on HP G8 Blade servers, with two 2.776 GHz processors that ran at 8 cores and three 8 GB DDR 3 1667 MHz RAM modules with STAR-CCM+ v.7.02.

4.3. Conclusion

This chapter described the detail, logic and reasoning behind the model setup. A discussion on both steady-state and transient multiphase simulations were presented. Details behind the geometry, mesh generation, model selection and model setup were presented. Sufficient information was provided to enable future studies to duplicate the results. The focus can subsequently be shifted to the results which were generated from the setup that have been discussed in this chapter.